INTERNATIONAL JOURNAL FOR NUMERICAL METHODS IN FLUIDS
Int. J. Numer. Meth. Fluids 2002; **40**:573–581 (DOI: 10.1002/fld.315)

Space-time residual distribution schemes for hyperbolic conservation laws on unstructured linear finite elements

Á. Csík[1,2,*] and H. Deconinck[1]

[1]*von Karman Institute for Fluid Dynamics, 72 Chaussée de Waterloo, 1640 Rhode-Saint-Genèse, Belgium*
[2]*Catholic University of Leuven, Center for Plasma Astrophysics, Celestijnenlaan 200B, B-3001 Herverlee, Belgium*

SUMMARY

Multidimensional upwind residual distribution schemes are extended to the context of continuous linear space–time finite elements for the time accurate solution of scalar and hyperbolic systems of conservation laws. The formulation leads to a consistent discretization of the space-time domain, thus retaining the properties of the underlying basic schemes both in space and time. We propose a particular space–time mesh configuration containing two layers of elements and three levels of nodes in time. This construction leads to unconditionally stable implicit time stepping while retaining second-order spatial and temporal accuracy in smooth flows and monotone solution across steep gradients. The presented schemes have a strong potential in the field of moving grids, since they allow a dynamic change of the space–time mesh geometry. Numerical results demonstrate the robustness, accuracy and monotonicity of the method. Copyright © 2002 John Wiley & Sons, Ltd.

KEY WORDS: time dependent; high resolution; multidimensional upwind schemes; space–time method; monotone shock capturing; unstructured grids

1. INTRODUCTION

In the last decade, a class of multidimensional upwind schemes has been developed for the solution of hyperbolic conservation laws on unstructured grids composed of linear finite elements. These schemes are based on the concept of residual distribution ($\mathfrak{RD}$), as first proposed by Ni, Morton and collaborators (see in Reference [1]). Upwinding and characteristic decomposition ideas have been incorporated by Roe, and further expanded by Roe, Deconinck, Abgral and their coworkers, see Reference [1] for a recent overview. Present $\mathfrak{RD}$ schemes for systems of equations are robust and second-order accurate in space for steady state problems. However, when combined with the method of lines (e.g. explicit Runge–Kutta time integration) to solve unsteady problems, space accuracy degrades to first order, similar to what occurs with stabilized finite elements when lumping the mass matrix. Several attempts have been made in the past to overcome this difficulty, using explicit Lax–Wendroff [2, 3]

*Correspondence to: Á. Csík, von Karman Institute for Fluid Dynamics, 72 Chaussée de Waterloo, 1640 Rhode-Saint-Genèse, Belgium.

Received May 2001
Revised October 2001

and implicit Cranck–Nicholson type schemes combined with a full mass matrix for the time dependent term [4]. In both approaches, a flux corrected transport method was used in order to have monotone discontinuity capturing, which is very unsatisfactory in the context of characteristic based upwind schemes.

The linear second-order (thus non-monotone) $\mathfrak{RD}$ schemes have been applied to large eddy simulation by Caraeni [5, 6], using a dual time stepping method. In his second-order time accurate implicit schemes the time dependent part of the residual is either upwinded in *space* along with the convective part, or discretized centrally. Unfortunately, due to the choice of discretization and distribution of the time dependent part of the residual, the monotonicity of the solution during the transient phase is not guaranteed.

Recently, Abgrall [1, 7] proposed to use the idea of a *continuous* space–time residual distribution to preserve the higher spatial and temporal accuracy of the basic $\mathfrak{RD}$ schemes. In two spatial dimensions the solution is represented by a bilinear interpolation over space–time on prismatic elements (triangular in space). The temporal slabs are naturally decoupled by limiting the distribution for a given prismatic element to the three nodes located forward in time. However, the schemes proposed by Abgrall, although being implicit, suffer from a severe time step restriction due to positivity requirements.

In the present contribution we employ the idea of a *continuous* space–time method, but we stay in the framework of linear simplicial finite elements, i.e. in 1D we apply the existing schemes to a triangulation of the space–time domain (tetrahedra for the case of two spatial dimensions). In order to decouple the solution onto temporal slabs allowing time-marching, the time step for a single-layer of the space–time elements has to satisfy a CFL restriction of order one, thus again severely limiting the time step. However, combining two layers in one implicit step allows unconditional stability for arbitrarily large time steps. The new method is second-order accurate both in space and time and extremely robust, at the price of a slightly-increased numerical dissipation originating from the time integration.

2. SPACE–TIME METHODS FOR HYPERBOLIC SYSTEMS IN ONE SPATIAL DIMENSION

We first consider the numerical solution of a 1D *scalar* conservation law over the space–time domain $\Omega = [x_L, x_R] \times [0, t_{\max}]$:

$$\boldsymbol{\nabla} \cdot \mathbf{F}(u) = 0 \quad \text{for } \forall (x,t) \in \Omega \tag{1}$$

where $\boldsymbol{\nabla} \equiv (\partial/\partial x, \partial/\partial t)$ is the Nabla operator in space–time, $\mathbf{F} = (F, u)$ is the flux vector with spatial and temporal components F and u, respectively, and $u(x,t)$ is the conserved quantity. The initial state is given as $u(x,0) = u_0(x)$.

We now apply previously developed residual distribution schemes [1] to solve the unsteady equation (1) on triangular elements in space–time, whereby no distinction is made between the temporal and spatial components of the flux at the level of the scheme. In general, this will lead to a coupled solution over the entire space–time domain. However, due to the upwinding property of the $\mathfrak{RD}$ schemes, a natural decoupling of the temporal slabs can be achieved for a well defined construction of the mesh, so that effectively a time marching method is obtained.

Recalling the basic idea of the $\mathfrak{RD}$ schemes we first consider a general space–time triangulation of the computational domain Ω. Assuming a piecewise linear variation of the solution

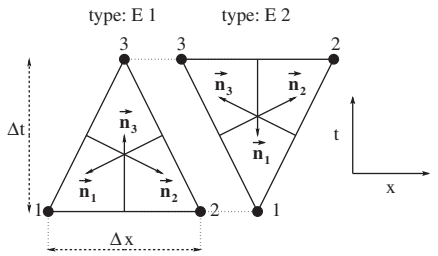

Figure 1. Space–time elements used in the 1D case.

u over each triangular element, integration of equation (1) over element E yields the definition of the total fluctuation or cell residual:

$$\phi^T = \int\int_E \nabla \cdot \mathbf{F}\, \mathrm{d}\Omega = \boldsymbol{\lambda} \cdot \int\int_E \nabla u\, \mathrm{d}\Omega \tag{2}$$

where $\boldsymbol{\lambda} = (a, 1) = (\partial F/\partial x, 1)$ is the linearized advection vector, taken to be cellwise constant. We assume that the linearization is conservative, i.e. the constant advection vector satisfies

$$\boldsymbol{\lambda} \cdot \int\int_E \nabla u\, \mathrm{d}\Omega = \oint_{\partial E} \mathbf{F} \cdot \mathbf{n}\, \mathrm{d}S \tag{3}$$

where the right-hand side is computed using a consistent contour integration. We consider weighted residual distribution schemes of the form

$$\phi_i = \sum_{E, i \in E} \phi_i^E = 0 \quad \text{for } \forall i \in (1, N) \tag{4}$$

where N is the total number of nodes of the mesh and ϕ_i^E is the contribution of element E to node i, given by $\phi_i^E = \beta_i^E \phi^T$. Here, β_i^E is the distribution coefficient, such that for a given triangle with local node numbers $\{1, 2, 3\}$ one has $\beta_1^E + \beta_2^E + \beta_3^E = 1$. System (4) represents a non-linear algebraic set of equations for the unknowns u_i, which can be solved by using a direct or iterative solver like Jacobi, Gauss Seidel or GMRES. In the present work we use explicit iteration in pseudo time to solve the implicit system for each physical time step. Typically, 10–50 explicit iterations are needed to converge the solution in pseudo time.

The multidimensional upwind property of the $\mathfrak{RD}$ schemes implies that the residual of a given cell only contributes to nodes which are *downstream* with respect to the constant advection speed vector $\boldsymbol{\lambda}$. A node in element E is defined to be downstream if the side opposed to this node sees an ingoing flux. Mathematically this is expressed by requiring that the corresponding upwinding parameter $k_i^E = \boldsymbol{\lambda} \cdot \mathbf{n}_i/2$ is positive, where $\mathbf{n}_i$ is the inward showing normal of the face opposite to node i, scaled with the length of the face (see Figure 1). Hence, all the schemes considered here are upwind in the sense that

$$\beta_i^E = 0 \quad \text{for } k_i^E \leqslant 0 \tag{5}$$

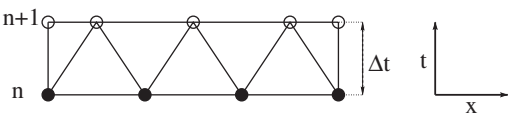

Figure 2. Schematic look of the mesh used in the 1D single-layer scheme.

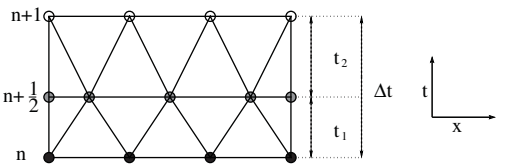

Figure 3. Schematic look of the mesh used in the 1D double-layer scheme.

Three different upwind schemes will be used in the present paper, as reviewed in Reference [1]:

- The linear N-scheme, which is positive and hence only first order.
- The linear LDA-scheme, which is second order and hence non-monotone.
- The monotone and second-order B-scheme, which is obtained by applying a non-linear blending between the N-scheme and the LDA-scheme.

2.1. Single-layer scheme

The *single-layer* scheme operates on a temporal slab with thickness Δt composed of one layer of space–time elements, with the nodes staggered in space between time levels n and $n+1$, as shown in Figure 2. The mesh consists of two types of elements (see also Figure 1). In order to decouple the temporal layers and allow time marching, nodes at level n must not receive any residual contribution from slab $[n, n+1]$, i.e. they have to satisfy $k_i \leqslant 0$. Since the temporal component of the advection vector is positive (equal to 1), this is always satisfied for triangles of type E_2. For triangles of type E_1, one obtains the simple CFL type condition:

$$\mathrm{CFL}_{E_1} = \left(\frac{|a|\Delta t}{\Delta x} \right)_{E_1} \leqslant \frac{1}{2} \quad \text{for all triangles of type } E_1 \tag{6}$$

allowing to determine the minimum as the global time step for the slab.

2.2. Double-layer scheme

The single-layer scheme, although being implicit, is subject to a severe time step limitation, as shown by Equation (6). To relax this constraint, we propose to impose the decoupling condition on a temporal slab consisting of two layers of elements, as shown in Figure 3. The first and second layers have a temporal width Δt_1 and Δt_2, respectively. Now the grid consists of three levels of nodes, denoted by n, $n+1/2$, and $n+1$. The CFL number for the

double layer scheme is given by

$$\mathrm{CFL} = \frac{|a|(\Delta t_1 + \Delta t_2)}{\Delta x} = \mathrm{CFL}_1\left(1 + \frac{\Delta t_2}{\Delta t_1}\right) = \mathrm{CFL}_1(1+Q) \tag{7}$$

where $\mathrm{CFL}_1 = |a|\Delta t_1/\Delta x$ is the CFL number for the first slab, required to satisfy condition (6) for all of its triangles of type E_1. However, no condition is required for Δt_2, hence an arbitrarily large CFL number can be obtained by increasing the value of the time step ratio $Q = \Delta t_2/\Delta t_1$, while maintaining unconditional stability. If a positive distribution scheme is used, such as the N-scheme or the B-scheme, monotonicity is preserved in space–time, while for the B-scheme and the LDA-scheme second-order accuracy in space and time is obtained. Applying a time marching with CFL larger than one can be very useful to overcome local time step restrictions due to very small cells in part of the domain, as will be shown in the results.

Note, that unlike in the case of the single-layer scheme, the solution at time level $n+1$ is obtained at the same spatial location as the solution at level n, while the solution at level $n+1/2$ is not used for the subsequent time marching step from $n+1$ to $n+2$.

2.3. *Extension to the system of Euler equations*

The method extends trivially to hyperbolic systems in one spatial dimension, by applying the *system* version of the upwind $\mathfrak{RD}$ schemes, see Reference [1] and the references therein. For the single-layer scheme, the marching (or decoupling) condition is obtained by requiring (6) to be satisfied for the largest eigenvalue of the Jacobian of the system, while for the double-layer scheme unconditional stability is obtained for arbitrarily high CFL number, if the marching condition is satisfied for the first layer. Applications to the Euler equations for a 1D unsteady shock tube and a quasi-1D steady nozzle flow will be shown in the results section.

3. EXTENSION TO TWO SPATIAL DIMENSIONS

Due to the lack of space, only the general ideas are presented here, more details will be provided in a future publication. Both the single- and double-layer schemes can be easily extended to two spatial dimensions, operating on tetrahedra using piecewise linear interpolation of the solution in space–time. Indeed, all upwind $\mathfrak{RD}$ schemes discussed before (N, LDA and B) extend trivially to tetrahedra (see Reference [1]), and the upwinding condition (5) remains valid, where the normal used in the definition of the upwind parameter k_i is now defined as the inward pointing face normal of the triangular face opposite to node i, scaled with the area of the face.

The arrangement proposed for the single-layer space–time mesh uses again a staggering in space, as shown in Figure 4. For the double-layer space–time scheme, the single-layer domain is mirrored, so that the spatial mesh at level $n+1$ is reduced to the spatial mesh at level n (which is an arbitrary triangulation of the spatial domain). Note that the arrangement of Figure 4 is not the only possible geometry, additional work is needed to study potentially more economic configurations (in terms of number of nodes). Considering the single-layer case, there are three types of tetrahedra, respectively with three (type E_1), two (type E_2)

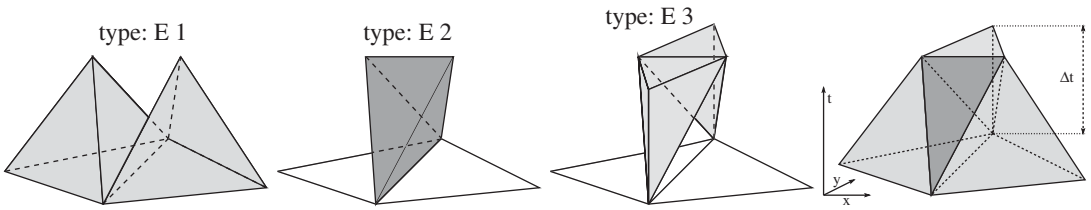

Figure 4. Three types of space–time elements used in the 2D single-layer geometry, and the schematic view of the space–time mesh.

and one (type E_3) node(s) located at level n. For tetrahedra of type E_3 no contribution of the residual is distributed to nodes at level n, while for tetrahedra of types E_1 and E_2 a decoupling condition can be derived by imposing Equation (5) for the nodes located at level n, leading again to an explicit-type CFL condition on the timestep. For the double-layer scheme, arbitrarily high CFL numbers can be used, if the marching condition is imposed on the first layer, just as before.

4. NUMERICAL RESULTS

Numerical results are shown for the double-layer scheme in one and two spatial dimensions. In the case of the Euler equations ρ, u, v, and p stand for the fluid density, components of the velocity in the x, y direction and pressure, respectively. The ratio of specific heats is $\gamma = 1.4$.

4.1. Verification of order of accuracy

In order to measure the order of accuracy of the presented $\mathfrak{RD}$ schemes, we perform two test cases in 1D with known analytic solution for four different mesh sizes, and compute the order of accuracy of the N, LDA and B schemes based on the L_2 norm of the numerical error.

The first test case is the problem of unsteady linear advection. The initial state is $u_0(x) = \sin(\pi x)$, for $x \in [-1, 1]$, and the advection speed is $a = 1$. The solution is computed at $t = 4$ by taking $Q = 1$ and global CFL $= 0.8$.

In the second test problem a fully supersonic steady solution of the quasi-1D nozzle flow is considered. The section of the nozzle is given by $S(x) = 1 + 1.5(1 - 0.2x)^2$ for $0 \leqslant x \leqslant 5$, and $S(x) = 1 + 0.5(1 - 0.2x)^2$ for $5 \leqslant x \leqslant 10$. The governing equations of this problem contain an algebraic source term in the momentum equation, which is proportional to p. This term is evaluated elementwise by a simple linear approximation, and distributed to the nodes in an upwind manner, consistently to the convective fluxes. In the initial state and at the supersonic inlet boundary we prescribe the following uniform state: $\rho = 0.14$, $u = 3$ and $p = 0.1$. In the simulations $Q = 1$ and CFL $= 0.99$ were taken.

The observed order of accuracy is summarized in Table I. The unsteady results indicate that the measured accuracy in space-time preserves the formal accuracy of the $\mathfrak{RD}$ schemes [1].

Table I. Measured order of accuracy of the N, LDA and B schemes.

Residual distribution scheme	N	LDA	B
Steady Q1D nozzle (density)	1.00	2.01	2.14
Unsteady linear advection	0.97	2.00	1.66

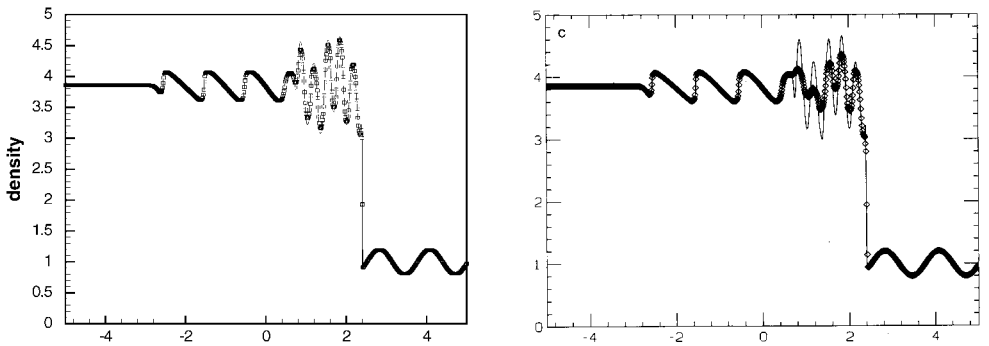

Figure 5. Shu–Oscher test case. Left: second-order monotone space–time B-scheme on 801 spatial nodes. Right: second-order MUSCL type finite volume scheme on 800 points [8].

4.2. *Shu–Osher shock tube problem*

To show the performance of the new method in one spatial dimension, we compute the oscillating Riemann problem proposed by Shu and Osher [8], corresponding to the propagation of a Mach 3 shock into a uniform domain superimposed by a sinusoidal density perturbation. The initial state is defined by $\rho_L = 3.857143$, $u_L = 2.629367$, $p_L = 10.333333$ for $x \leqslant -4$ and $\rho_R = 1 + 0.2\sin(5x)$, $u_R = 0$, $p_R = 1$ for $x > -4$. In the computation we use $Q = 2$ and CFL $= 1.49$. The solution at $t = 1.8$ is shown in the left of Figure 5 for a mesh with 801 nodes in the spatial direction computed by the non-linear second-order monotonicity preserving B-scheme. The solid line corresponds to a solution on a mesh containing 1601 spatial nodes. In the right of Figure 5, a second-order computation done by Shu and Osher is shown using a MUSCL type finite volume scheme on 800 points [8].

4.3. *Mach 3 wind tunnel with a forward facing step*

To illustrate the performance of the new schemes for an unsteady flow in two spatial dimensions, we compute the test case proposed by Colella and Woodward [9]. The spatial mesh is a uniform triangulation of the domain with average size of the triangles given by $h = 1/80$, except for the corner of the step, where a severe local refinement was used, as shown in Figure 6. This refinement is necessary to limit the numerical entropy production at the corner, see also Reference [10] for more details. In total the spatial mesh has 38 740 triangles and 19 715 nodes.

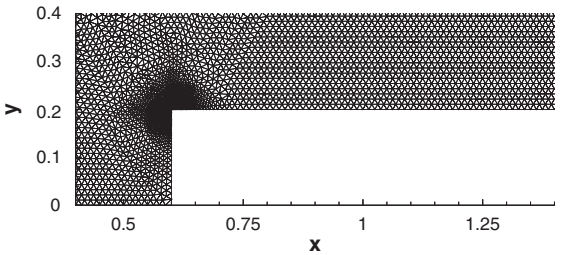

Figure 6. Part of the unstructured spatial grid used for the space–time computation.

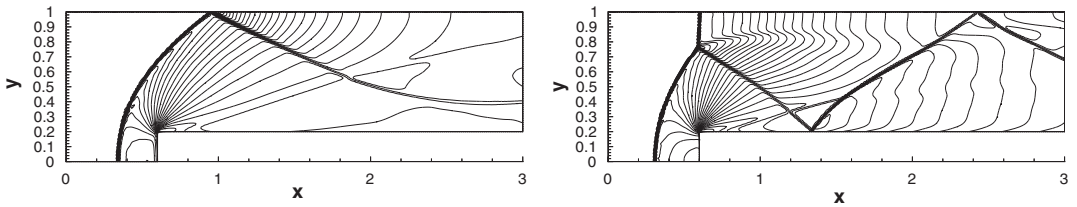

Figure 7. Mach 3 flow over a forward facing step, non-linear second-order space–time B-scheme. Left: $t = 1.0$, right: $t = 4.0$.

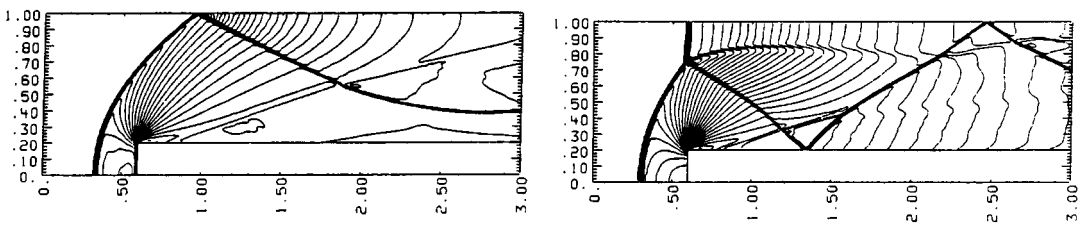

Figure 8. Mach 3 flow over a forward facing step. Reference solution: third-order PPM scheme on Cartesian mesh [9]. Left: $t = 1.0$, right: $t = 4.0$.

The computation is made with the non-linear B-scheme using the double-layer approach on space–time tetrahedra. The global timestep is chosen such that CFL ≈ 1 for the triangles in the uniform region. However, in the corner region this amounts to a local value of CFL ≈ 12, due to the small size of the cells in this area. This clearly shows the benefit of an unconditionally stable scheme, even for unsteady computations.

Isolines of the density at different instances in time are presented in Figure 7 and compared with the solution of Reference [9] (see Figure 8). This reference solution is computed with a third-order PPM method on a uniform mesh with square cells of size $h = 1/80$.

5. CONCLUSIONS

In the present paper existing steady $\mathfrak{RD}$ schemes have been extended to the context of linear space–time elements for the time-accurate solution of conservation laws. We proposed a *double-layer* variant of the method allowing arbitrary physical time steps, while retaining unconditional stability if a CFL like condition is respected by the temporal width of the first layer in the mesh. At the same time the method is guaranteed second-order and monotone in space–time, inheriting the properties of the underlying steady schemes. Using high CFL numbers is particularly important if the mesh contains highly refined regions, e.g. around corners. This is also the case for Navier–Stokes computations, where the small mesh size in the boundary layer constrains the time step much more than the physical time scale of interest.

Like in the case of any implicit time integration method allowing high CFL numbers, one physical time step requires the solution of an implicit system of equations. In the present approach the full space–time mesh contains approximately four times the unknowns of the spatial grid, for the case of the *double-layer* scheme in two spatial dimensions. This is a substantial overhead compared to classical approaches, and it has to be balanced by improved accuracy, monotonicity and stability. A detailed comparison is beyond the scope of this paper and is the subject of future work.

On the other hand, the space–time $\mathfrak{RD}$ method proposed here has strong potential in the field of applications involving moving boundaries. Since the second and the third levels of nodes may have different spatial co-ordinates than the nodes at the first level, the number of grid points and spatial positions can dynamically change in time, while retaining full conservation, monotonicity and higher order accuracy in both space and time.

ACKNOWLEDGEMENTS

The authors gratefully acknowledge the contribution of M. Ricchiuto in many discussions on the space–time approach, and for the 2D test computation he performed. We thank A. Athanasiadis for the generation of the mesh for the Mach 3 wind tunnel testcase.

REFERENCES

1. Deconinck H, Sermeus K, Abgrall R. Status of multidimensional upwind residual distribution schemes and applications in aeronautics. *AIAA CP* 2000-2328, 2000.
2. Hubbard ME, Roe PL. Compact high-resolution algorithms for time-dependent advection on unstructured grids. *International Journal for Numerical Methods in Fluids* 2000; **33**(5):711–736.
3. Ricchiuto M, Deconinck H. Time accurate solution of hyperbolic partial differential equations using fct and residual distribution. *Stagiaire Report* 1999-33, von Karman Institute, 1999.
4. Ferrante A, Deconinck H. Solution of the unsteady Euler equations using residual distribution and flux corrected transport. *Project Report* 1997-08, von Karman Institute, 1997.
5. Caraeni DA. Development of a multidimensional residual distribution solver for large eddy simulation of industrial turbulent flows. *Ph.D. Thesis*, Lund Institute of Technology, 2000.
6. Caraeni DA, Caraeni M, Fuchs L. A parallel multidimensional upwind algorithm for les (i). *AIAA CP* 2001-2547, 2001.
7. Abgrall R, Mezine M. A consistent upwind residual scheme for unsteady advection problems. *Presented at 2nd ESF AMIF Conference*, Tuscany, Italy, 2000.
8. Shu CW, Osher S. Efficient implementation of essentially non-oscillatory shock capturing schemes. *Journal of Computational Physics* 1989; **83**(1):32–78.
9. Colella P, Woodward P. The numerical simulation of two-dimensional fluid flow with strong shocks. *Journal of Computational Physics* 1984; **54**(1):115–173.
10. Cockburn B. Discontinuous Galerkin methods for convection-dominated problems. In *High-Order Methods for Computational Physics*, Barth TJ, Deconinck H (eds). Springer: Berlin, 1999; 69–224.

